Inorg. Chem. **2007**, *46*, 8044–8050

Carbon–Sulfur Bond Formation via Alkene Addition to an Oxidized Ruthenium Thiolate

Craig A. Grapperhaus,* Kiran B. Venna, and Mark S. Mashuta

Department of Chemistry, University of Louisville, Louisville, Kentucky 40292

Received June 1, 2007

Bulk oxidation of [Ru(DPPBT)$_3$], **1b**, (DPPBT = 2-diphenylphosphinobenzenethiolate) in the presence of ethylene yields [(ethane-1,2-diylbis(thio-2,1-phenylene)diphenylphosphine) ruthenium(II)] hexafluorophosphate, **[2a]PF$_6$**, from the addition of the alkene across cis sulfur sites. During oxidation, the absorption bands of **1b** at 540, 797, and 1041 nm decrease in intensity. The resulting complex **[2a]**$^+$ displays a single redox couple at +804 mV. The +ESI-MS of **[2a]**$^+$ shows a parent ion peak at m/z = 1009.1013, and the ^{31}P NMR spectrum displays chemical shift values of δ_1 = 61.0, δ_2 = 40.3, and δ_3 = 37.5 with coupling constants of $J_{12} \approx J_{13} \approx$ 30 Hz and J_{23} = 304 Hz. Oxidation of **[2a]**$^+$ by one electron at a holding potential of +1000 mV yields [(ethane-1,2-diylbis(thio-2,1-phenylene)diphenyl phosphine)ruthenium(III)] hexafluorophosphate, **[2b][PF$_6$]$_2$**. The EPR of **[2b][PF$_6$]$_2$** displays a rhombic signal with g_1 = 2.09, g_2 = 2.04, and g_3 = 2.03. Oxidation of **1b** in the presence of alkenes including 1-hexene, styrene, cyclohexene, and norbornene yields products similar to **[2a]**$^+$. Each of these products was further oxidized to an analogue of **[2b]**$^{2+}$. Complex **[2a]**$^+$ was also prepared, as the bromide salt, from [PPN][Ru(DPPBT)$_3$] (**PPN [1a]**; PPN = bis(triphenylphosphoranylidene)ammonium) and 1,2-dibromoethane. The complex **[2a]Br** crystallizes as thin yellow plates in the monoclinic space group $P2_1/c$ with unit cell dimensions of a = 10.2565(9) Å, b = 13.2338(12) Å, c = 38.325(3) Å, and β = 93.3960(10)°.

Introduction

Sulfenyl radicals, also commonly referred to as thiyl radicals, are organosulfur compounds with the general formula RS$^\bullet$. The reactivity of thiyl radicals with organic compounds can be consolidated into three major categories: disulfide formation, H-atom abstraction, and addition to unsaturated compounds.[1] Oxidation of metal thiolates to disulfides is well known and is often suspected as the aerobic decomposition pathway.[2,3] Recently, much effort has been directed toward the stabilization and characterization of metal-coordinated thiyl radicals.[4] In contrast to metal-coordinated phenoxyl radicals, metal-coordinated phenylthiyl radicals tend to delocalize the unpaired electron density over the metal−sulfur bond.[5] As such, metal-coordinated thiyl radicals can be stabilized by sufficiently bulky groups that prevent disulfide formation, thereby opening alternate reaction pathways.

The H-atom abstraction path is limited for organic thiyl radicals by the relatively weak S−H bond of the thiol product. As such, thiyl radicals can only abstract H atoms from activated carbon centers, such as the 3′ carbon of the ribose unit in ribonucleotides.[6] In ribonucleotide reductase (RNR), metal cofactors assist in the generation of a *non-coordinated* thiyl radical, which initiates reduction of the ribose unit.[6] However, *metal-coordinated* thiyl radicals have an even more limited utility for H-atom abstraction, as metal coordination stabilizes the radical and destabilizes the S−H bond of the product.

The addition of organic thiyl radicals to unsaturated hydrocarbons in C−S bond-forming reactions is well known, with applications for cis/trans isomerization, sulfide synthesis, and polymerization.[7−10] Alkene addition to oxidized metal−

* To whom correspondence should be addressed. E-mail: grapperhaus@louisville.edu. Phone: (502)852-5932. Fax: (502)852-8149.

(1) Alfassi, Z. B. *S-centered radicals*. John Wiley and Sons: Chichester, 1999.
(2) Treichel, P. M.; Rosenhein, L. D. *Inorg. Chem.* **1984**, *23*, 4018−4022.
(3) (a) Albela, B.; Bothe, E.; Brosch, O.; Mochizuki, K.; Weyhermuller, T.; Wieghardt, K. *Inorg. Chem.* **1999**, *38*, 5131−5138. (b) Díaz, C.; Araya, E.; Santa Ana, M. A. *Polyhedron* **1998**, *17*, 2225−2230.
(4) Ray, K.; Petrenko, T.; Wieghardt, K.; Neese, F. *J. Chem. Soc. Dalton Trans.* **2007**, 1552−1566.
(5) Kimura, S.; Bill, E.; Bothe, E.; Weyhermuller, T.; Wieghardt, K. *J. Am. Chem. Soc.* **2001**, *123*, 6025−6039.
(6) Stubbe, J. A.; van der Donk, W. A. *Chem. Rev.* **1998**, *98*, 705−762.
(7) Walling, C.; Helmreich, W. *J. Am. Chem. Soc.* **1958**, *81*, 1144−1148.

10.1021/ic701078e CCC: $37.00
Published on Web 08/17/2007

Scheme 1

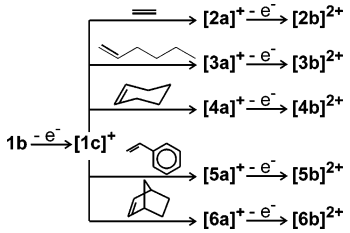

sulfur complexes has been previously reported, although a metal-coordinated thiyl radical was not invoked. The addition of alkenes to an oxidized nickel dithiolene was reported by Stiefel, although later studies revealed the reactivity was more complex, vide infra.[11−13] Recently, Webster, Goh, and coworkers reported reported the addition of acrylonitrile to a ruthenium thiolate upon chemical oxidation.[14]

Previous results from our laboratory have shown that oxidation of $[Ru(DPPBT)_3]^-$ (**[1a]**$^-$) (DPPBT = 2-diphenylphosphinobenzenethiolate) proceeds in two one-electron steps.[15] The first oxidation yields the neutral complex **1b**, which has a Ru(III)−thiolate ground state with Ru(II)−thiyl radical contributions. The second oxidation yields a reactive intermediate $[Ru(DPPBT)_3]^+$, **[1c]**$^+$. On the basis of recent DFT investigations, **[1c]**$^+$ is best described as having a singlet diradical ground state with significant Ru(II)−dithiyl radical character.[16] The two unpaired electrons sit in nearly orthogonal orbitals, which significantly retards disulfide formation.[15] In the presence of methyl ketones, **[1c]**$^+$ reacts with the enol tautomer to generate Ru(II)−thioether complexes.[17] In this manuscript, we further report the reaction of **[1c]**$^+$ with a variety of alkenes. As shown in Scheme 1, ethylene, 1-hexene, cyclohexene, styrene, and norbornene have been successfully added to **[1c]**$^+$ to generate a series of Ru(II)−dithioether complexes, **[2a]**$^+$−**[6a]**$^+$. Preliminary studies with styrene were previously communicated.[16] Each complex can be further oxidized to the Ru(III) analogue, **[2b]**$^{2+}$−**[6b]**$^{2+}$. Complex **[2a]**$^+$ has been isolated as the bromide salt for X-ray crystallographic analysis.

Experimental Section

Materials and Reagents. Solvents were purified and dried using standard procedures. All chemical reagents were commercially obtained and used without further purification. The complex [PPN]-$[Ru(DPPBT)_3]$ **[1a]**$^-$ was synthesized according to published procedures and was stored in a nitrogen atmosphere dry box.[18] The neutral $[Ru(DPPBT)_3]$ complex, **1b**, was generated electrochemically immediately before use as described previously.[15] Deuterated solvents required for NMR experiments were purchased from Cambridge Isotope Laboratories and used without further purification. All reactions were conducted under anaerobic conditions by using standard Schlenk techniques, unless otherwise specified.

Physical Methods. NMR spectra were recorded on a Varian 500 MHz spectrometer and referenced to TMS (^{1}H NMR) or 85% phosphoric acid (^{31}P NMR). For electrochemically generated complexes, ^{31}P NMR samples were prepared by removal of solvent under vacuum and extraction of the analyte into deuterated acetonitrile. The sample was filtered through the fritted septa of 13 mm syringe filter with a 0.2 μm PTFE membrane into the NMR tube. Electron paramagnetic resonance spectra were collected on a Bruker EMX EPR spectrometer at 77 K in a Suprasil quartz dewar. EPR data were simulated using SimPow6.[19] Electrospray ionization (ESI) mass spectra were recorded at the Mass Spectrometry Application and Collaboration Facility in the Chemistry Department at Texas A&M University. An Agilent 8453 diode-array spectrometer was used for electronic absorbance measurements.

Electrochemical Methods. All electrochemical experiments were performed with an EG&E 273 potentiostat. Potentials are reported versus a Ag/AgCl reference electrode for which the ferrocenium/ferrocene redox couple was observed at +460 mV. Electrochemical and spectroelectrochemical experiments were performed in a custom cell designed by E. Böthe of Max-Planck Institute für Bioanorganische Chemie, Mülheim, Germany. The cell has a quartz window with a path length of 0.5 cm and variable-temperature jacketed sample holder. The cell was connected to a VWR 1190A chiller that was set at −34 °C and produced a temperature of −22 ± 3 °C in the cell. All the measurements were taken at the above-mentioned temperature unless noted otherwise. To avoid condensation on the cell during low-temperature conditions, the cell holder was placed in a Plexiglas box fitted with Dynasil 4000 quartz windows (Pacific Quartz), through which nitrogen gas was purged. Coulometric and electronic absorption measurements were done simultaneously with 10 mL of acetonitrile as solvent and 0.100 M tetrabutylammonium hexafluorophosphate (TBAHFP) as supporting electrolyte. The electrochemical cell was purged with nitrogen to prevent oxygen diffusion and also to ensure thorough solution mixing. For coulometric measurements, a platinum mesh was used as working electrode with a Ag^0/Ag^+ as the reference electrode. After each oxidation, a glassy carbon electrode was used to record the square-wave voltammogram (frequency = 60 Hz, pulse height = 0.025 V).

Chemical Method Synthesis of [(Ethane-1,2-diylbis(thio-2,1-phenylene)diphenylphosphine)ruthenium(II)] Bromide ([2a]Br). To a 50 mL Schlenk flask was added 0.092 g (0.061 mmol) of **PPN[1a]** and 17 mL of chlorobenzene. The solution was stirred for 10 min, and then 8.4 μL (0.097 mmol) of 1,2-dibromoethane was added. The resulting solution was stirred overnight during which time a dark red color developed. The mixture was then filtered through Celite, and the dark red filtrate was layered with diethyl ether to yield **[2a]Br** as yellow crystals. Yield: 0.0354 g (54.7%). $E_{1/2}$ (Ru^{III}/Ru^{II}) = +794 mV. +ESI-MS for $C_{56}H_{46}P_3S_3Ru$: experimental = 1009.1015 amu, theoretical = 1009.1018 amu.

Electrochemical Method Synthesis of [(Ethane-1,2-diylbis-(thio-2,1-phenylene)diphenylphosphine)ruthenium(II)] Hexafluorophosphate ([2a]PF_6). In the custom-designed spectroelectrochemical cell containing 0.100 M TBAHFP, 10.0 mL of a 1.3 mM

(8) Chatgilialoglu, C.; Ferreri, C.; Ballestri, M.; Mulazzani, Q. G.; Landi, L. *J. Am. Chem. Soc.* **2000**, *122*, 4593−4601.
(9) Ichinose, Y.; Oshima, K.; Utimoto, K. *Chem. Lett.* **1988**, 669−672.
(10) Lalevee, J.; Allonas, X.; Fouassier, J. P. *J. Org. Chem.* **2006**, *71*, 9723−9727.
(11) Wang, K.; Stiefel, E. I. *Science* **2001**, *291*, 106−109.
(12) Geiger, W. E. *Inorg. Chem.* **2002**, *41*, 136−139.
(13) Harrison, D. J.; Nguyen, N.; Lough, A. J.; Fekl, U. *J. Am. Chem. Soc.* **2006**, *128*, 11026−11027.
(14) Shin, R. Y. C.; Teo, M. E.; Leong, W. K.; Vittal, J. J.; Yip, J. H. K.; Goh, L. Y.; Webster, R. D. *Organometallics* **2005**, *24*, 1483−1494.
(15) Grapperhaus, C. A.; Poturovic, S. *Inorg. Chem.* **2004**, *43*, 3292−3298.
(16) Grapperhaus, C. A.; Kozlowski, P. M.; D., K.; Frye, H. N.; Venna, B. K.; Poturovic, S. *Angew. Chem., Int. Ed.* **2007**, 4085-4088.
(17) Poturovic, S.; Mashuta, M. S.; Grapperhaus, C. A. *Angew. Chem., Int. Ed.* **2005**, *44*, 1883−1887.
(18) Grapperhaus, C. A.; Poturovic, S.; Mashuta, M. S. *Inorg. Chem.* **2002**, *41*, 4309−4311.
(19) Nilges, M. J. *Simpow6*.

solution of **1b** was prepared immediately before use at −22 ± 3 °C. Ethylene gas was then purged through the solution during which time a potential of +0.620 V was applied. Oxidation of the mixture generated a light yellow solution. After ~1049 mC (0.83 electron equiv) of charge production, the current decayed to background levels. The resulting solution contained **[2a]**$^+$. $E_{1/2}$ (Ru^{III}/Ru^{II}) = +804 mV. +ESI-MS for $C_{56}H_{46}P_3S_3Ru$: experimental = 1009.1013 amu, theoretical = 1009.1018 amu.

Electrochemical Method Synthesis of [(Ethane-1,2-diylbis-(thio-2,1-phenylene)diphenylphosphine)ruthenium(III)] Hexafluorophosphate ([2b][PF$_6$]$_2$). In the custom-designed spectroelectrochemical cell, a potential of +1.00 V was applied to a freshly prepared solution of **[2a]**$^+$ (~1 mM) at −22 ± 3 °C until the current decayed to background levels. A green-colored solution of **[2b]-[PF$_6$]$_2$** was obtained after oxidation by 1326 mC (1.05 electron equiv). Electronic absorption: λ_{max} (ϵ, cm^{-1} M^{-1}): 690 nm (3800). EPR: g = 2.09, 2.04, and 2.03. **[2b]**$^{2+}$ can be reduced to **[2a]**$^+$ at an applied potential < +800 mV.

Electrochemical Synthesis of [(Hexane-1,2-diylbis(thio-2,1-phenylene)diphenylphosphine)ruthenium(II)] Hexafluorophosphate ([3a]PF$_6$). Complex **[3a]**$^+$ was generated in a manner analogous to **[2a]**$^+$ with the following exceptions. Prior to oxidation, 2.0 mL (16 mmol) of 1-hexene was added and during oxidation the solution was purged with N_2 in place of ethylene. $E_{1/2}$ (Ru^{III}/Ru^{II}) = +792 mV. +ESI-MS for $C_{60}H_{54}P_3S_3Ru$: experimental = 1065.1655 amu, theoretical = 1065.1643 amu.

Electrochemical Synthesis of [(Hexane-1,2-diylbis(thio-2,1-phenylene)diphenylphosphine)ruthenium(III)] Hexafluorophosphate ([3b][PF$_6$]$_2$). Complex **[3b][PF$_6$]$_2$** was generated in a manner analogous to **[2b][PF$_6$]$_2$**. $E_{1/2}$ (Ru^{III}/Ru^{II}) = +798 mV. Electronic absorption: λ_{max} (ϵ, cm^{-1} M^{-1}): 682 nm (2700). EPR: g = 2.08, 2.03, and 2.02. **[3b]**$^{2+}$ can be reduced to **[3a]**$^+$ at an applied potential < +800 mV.

Electrochemical Synthesis of [(Cyclohexane-1,2-diylbis(thio-2,1-phenylene)diphenylphosphine)ruthenium(II)] Hexafluorophosphate ([4a]PF$_6$). Complex **[4a]**$^+$ was generated in a manner analogous to **[2a]**$^+$ with the following exceptions. Prior to oxidation, 2.0 mL (20 mmol) of cyclohexene was added and during oxidation the solution was purged with N_2 in place of ethylene. $E_{1/2}$ (Ru^{III}/Ru^{II}) = +790 mV. ESI-MS for $C_{60}H_{52}P_3S_3Ru$: experimental = 1063.1493 amu, theoretical =1063.1487 amu.

Electrochemical Synthesis of [(Cyclohexane-1,2-diylbis(thio-2,1-phenylene)diphenylphosphine)ruthenium(III)] Hexafluorophosphate ([4b][PF$_6$]$_2$). Complex **[4b][PF$_6$]$_2$** was generated in a manner analogous to **[2b][PF$_6$]$_2$**. $E_{1/2}$ (Ru^{III}/Ru^{II}) = +782 mV. Electronic absorption: λ_{max} (ϵ, cm^{-1} M^{-1}): 697 (2500). EPR: g = 2.09, 2.05, 2.02. **[4b]**$^{2+}$ can be reduced to **[4a]**$^+$ at an applied potential < +800 mV.

Electrochemical Synthesis of [(Phenylethane-1,2-diylbis(thio-2,1-phenylene)diphenylphosphine)ruthenium(II)] Hexafluorophosphate ([5a]PF$_6$). Complex **[5a]**$^+$ was generated in a manner analogous to **[2a]**$^+$ with the following exceptions. Prior to oxidation, 2.0 mL (17 mmol) of styrene was added and during oxidation the solution was purged with N_2 in place of ethylene. $E_{1/2}$ (Ru^{III}/Ru^{II}) = +788 mV. +ESI-MS for $C_{62}H_{50}P_3S_3Ru$: experimental = 1085.1318 amu, theoretical = 1085.1331 amu.

Electrochemical Synthesis of [(Phenylethane-1,2-diylbis(thio-2,1-phenylene)diphenylphosphine)ruthenium(III)] Hexafluorophosphate ([5b][PF$_6$]$_2$). Complex **[5b][PF$_6$]$_2$** was generated in a manner analogous to **[2b][PF$_6$]$_2$**. $E_{1/2}$ (Ru^{III}/Ru^{II}) = +808 mV. Electronic absorption: λ_{max} (ϵ, cm^{-1} M^{-1}): 692 nm (2200). EPR: g = 2.09, 2.05, 2.03. **[5b]**$^{2+}$ can be reduced to **[5a]**$^+$ at an applied potential < +800 mV.

Electrochemical Synthesis of [(Norbornane-1,2-diylbis(thio-2,1-phenylene)diphenylphosphine)ruthenium(II)] Hexafluorophosphate ([6a]PF$_6$). Complex **[6a]**$^+$ was generated in a manner analogous to **[2a]**$^+$ with the following exceptions. Prior to oxidation, 0.100 g (1.06 mmol) of norbornene was added and during oxidation the solution was purged with N_2 in place of ethylene. $E_{1/2}$ (Ru^{III}/Ru^{II}) = +824 mV. +ESI-MS for $C_{61}H_{52}P_3S_3Ru$: experimental = 1075.1478 amu, theoretical = 1075.1487 amu.

Electrochemical Synthesis of [(Norbornane-1,2-diylbis(thio-2,1-phenylene)diphenylphosphine)ruthenium(III)]Hexafluorophosphate ([6b][PF$_6$]$_2$). Complex **[6b][PF$_6$]$_2$** was generated in a manner analogous to **[2b][PF$_6$]$_2$**. Electronic absorption was not determined due to precipitation **[6b][PF$_6$]$_2$** during oxidation. EPR: g = 2.09, 2.05, 2.03. **[6b]**$^{2+}$ can be reduced to **[6a]**$^+$ at an applied potential < +800 mV.

Crystallographic Studies. A thin yellow plate 0.41 × 0.27 × 0.07 mm^3 crystal of **[2a]Br** was mounted on a 0.05 mm CryoLoop with Paratone oil for collection of X-ray data on a Bruker SMART APEX CCD diffractometer. The SMART[20] software package (v 5.628) was used to acquire a total of 1868 30-s frame ω-scan exposures of data at 100 K to a 2θ max = 56.16° using monochromated Mo Kα radiation (0.71073 Å) from a sealed tube and a monocapillary. Frame data were processed using SAINT[21] (v 6.36) to determine final unit cell parameters a = 10.2565(9) Å, b = 13.2338(12) Å, c = 38.325(3) Å, α = 90°, β = 93.3960(10)°, γ = 90°, V = 5192.8(8) $Å^3$, Z = 4, and ρ_{calcd} = 1.501 Mg m^{-3} to produce raw *hkl* data that were then corrected for absorption (transmission min/max = 0.65/0.91; μ = 1.364 mm^{-1}) using SADABS[22] (v 2.02). The structure was solved by Patterson methods in the monoclinic space group $P2_1/c$ using SHELXS-90[23] and refined by least-squares methods on F^2 using SHELXL-97[24] incorporated into the SHELXTL[25] (v 6.12) suite of programs. All non-hydrogen atoms were refined anisotropically. Phenyl H's were calculated and assigned U(H) = 1.2U_{eq}. For 12,095 unique reflections (R(int) = 0.043), the final anisotropic full matrix least-squares refinement on F^2 for 610 variables converged at R1 = 0.0504 and wR2 = 0.1164 with a GOF of 1.097. Details of data collection, structure solution, and refinement are given in Table 1.

Results

Synthesis. A series of dithioether/thiolate ruthenium(II) complexes were prepared upon the one-electron oxidation of $Ru^{III}(DPPBT)_3$ (**1b**) in the presence of various alkenes, Scheme 1. The alkenes employed include ethylene, 1-hexene, cyclohexene, styrene, and norbornene. Preliminary details for the preparation of **5a** have been previously reported.[16] Each of the Ru(II) addition products (**[2a]**$^+$−**[6a]**$^+$) were further oxidized electrochemically to the Ru(III) derivative (**[2b]**$^{2+}$−**[6b]**$^{2+}$). A detailed description of the oxidation of **1b** in the presence of ethylene to generate **[2a]**$^+$ and its subsequent oxidation to **[2b]**$^{2+}$ is provided below. The related

(20) *SMART (v.5.628)*; Bruker Advanced X-ray Solutions, Inc.: Madison, WI, 2002.
(21) *SAINT (v6.36)*; Bruker Advanced X-ray Solutions, Inc.: Madison, WI, 2002.
(22) Sheldrick, G. M. *SADABS (v2.02)*; University Göttingen: Göttingen, Germany, 2001.
(23) Sheldrick, G. M. *SHELXS-90*, A46; University of Göttingen: Göttingen, Germany, 1990.
(24) Sheldrick, G. M. *SHELXL-97*; University Göttingen: Göttingen, Germany, 1997.
(25) *SHELXTL (v6.12)*; Bruker Advanced X-ray Solutions, Inc.: Madison, WI, 2001.

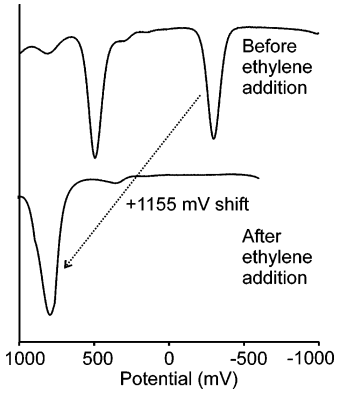

Figure 1. Square-wave voltammogram of **1b** (top) and **[2a]**$^+$ (bottom) recorded in acetonitrile with 0.1M TBAHFP at −20 °C. Potentials referenced to Ag/AgCl.

Table 1. Crystal Data and Structure Refinement for **[2a]Br**

empirical formula	$C_{56}H_{46}BrP_3RuS_3 \cdot 0.75C_6H_5Cl$
fw	1173.41
temp	100(2) K
wavelength (Å)	0.71073
space group	$P2_1/c$
unit cell dimens	
a, (Å)	10.2565(9)
b, (Å)	13.2338(12)
c, (Å)	38.325(3)
β, (°)	93.3960(10)
vol, (Å^3)	5192.8(8)
Z	4
density, (Mg m^{-3})	1.501
abs coeff (mm^{-1})	1.364
cryst size (mm^3)	0.41 × 0.27 × 0.07
cryst color, habit	yellow plate
θ range for data collection (°)	1.87−28.08
index ranges	$-13 \le h \le 12$
	$-17 \le k \le 17$
	$-50 \le l \le 50$
reflns collected	44 978
indep reflns	12 095 [R(int) = 0.043]
completeness to $\theta = 28.08°$	95.6%
abs correction	SADABS
min and max transm	0.65 and 0.91
refinement method	full-matrix least-squares on F^2
data/restraints/params	12 095/0/610
GOF on F^2	1.097
final R indices [$I > 2\sigma(I)$][a,b]	R1 = 0.0504, wR2 = 0.1164
R indices (all data)[a,b]	R1 = 0.0646, wR2 = 0.1215
largest peak and hole (e Å^{-3})	1.456 and −0.936

[a] $R1 = \sum||F_o| - |F_c||/\sum|F_o|$. [b] $wR2 = \{\sum[w(F_o^2 - F_c^2)^2]^2/\sum[w(F_o^2)^2]\}^{1/2}$.

complexes **[3a]**$^+$/**[3b]**$^{2+}$−**[6a]**$^+$/**[6b]**$^{2+}$ were prepared in an analogous manner.

The precursor complex, **1b**, was freshly prepared by bulk oxidation of **[1a]**$^-$ at an applied potential of +100 mV in acetonitrile at −20 °C as described previously.[15] The square-wave voltammogram of **1b** is shown in Figure 1 (top). Complex **1b** was oxidized by one electron to **[1c]**$^+$ at an applied potential of +620 mV while ethylene gas was purged continuously through the solution. As shown in Figure 2, a trace of the UV−visible spectra recorded during the oxidation reveals a decrease in intensity of the bands of **1b** at 540, 797, and 1041 nm. After a complete one-electron oxidation, the spectra did not further change and the current dropped to background levels. It is important to note that the characteristic absorbance band of **[1c]**$^+$, at 850 nm, is not

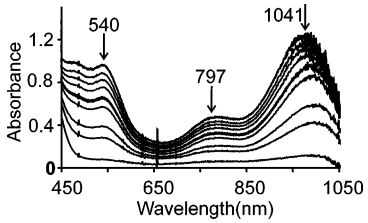

Figure 2. Electronic spectra obtained during oxidation of **1b** in the presence of ethylene. Spectra were obtained on a 1.13 mM acetonitrile solution approximately every one-tenth of an electron equivalent at −20 °C.

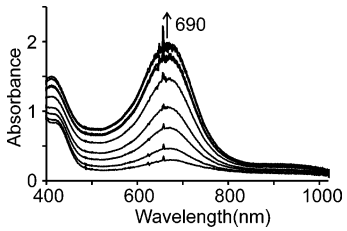

Figure 3. Electronic spectra obtained during oxidation of **[2a]**$^+$ to **[2b]**$^{2+}$. Spectra were obtained on a 1.13 mM acetonitrile solution approximately every one-tenth of an electron equivalent at −20 °C.

observed during the oxidation.[15] This is consistent with a rapid reaction between **[1c]**$^+$ and ethylene. In the absence of an appropriately applied potential, **1b** is unreactive with ethylene gas.

The square-wave voltammogram of **[2a]**$^+$, Figure 1 (bottom), reveals a single event at +804 mV assigned as a $Ru^{III/II}$ couple. Importantly, no other redox events are observed. The observed potential is shifted by +1155 mV from the $Ru^{III/II}$ couple of **1b** and is similar to that of the related dithioether/thiolate ruthenium(II) complex, [(methane-1,2-diylbis(thio-2,1-phenylene)diphenylphosphine)ruthenium-(II)] (**[7a]Cl**).[18] The potential is also similar to that of the disulfide product obtained upon oxidation of **1b** in acetonitrile.[15] However, the disulfide complex is thermally unstable and degrades to a complex mixture upon warming to room temperature, while solutions of **[2a]**$^+$ are stable at room temperature for several weeks with no notable changes in spectroscopic properties.

Complex **[2a]**$^+$ was oxidized to its Ru(III) derivative, **[2b]**$^{2+}$, at an applied potential of +1000 mV. The charge produced during the reaction is consistent with a one-electron oxidation per ruthenium. The square-wave voltammogram recorded following oxidation of **[2b]**$^{2+}$ is indistinguishable from **[2a]**$^+$, as expected. A UV−visible trace recorded during the oxidation, Figure 3, shows a rise in intensity at λ_{max} = 690 nm which can be assigned as a thiolate-to-metal charge-transfer band, consistent with a Ru(III) oxidation state. Solutions of **[2b]**$^{2+}$ can be oxidized back to **[2a]**$^+$ at an applied potential < +804 mV.

The oxidation of **1b** in the presence of other alkenes also proceeds via a one-electron oxidation followed by a chemical step resulting in alkene addition to yield complexes **[3a]**$^+$−**[6a]**$^+$. Further oxidation at +1000 mV yields the corresponding derivatives, **[3b]**$^{2+}$−**[6b]**$^{2+}$.

The dithioether/thiolate ruthenium(II) complex, **[2a]**$^+$, can also be prepared in the direct chemical reaction of **[1a]**$^-$ and

Table 2. Properties of Ru(II)−Dithioether Complexes **[2a]**$^+$−**[6a]**$^+$

	[2a]$^+$	**[3a]**$^+$	**[4a]**$^+$	**[5a]**$^+$	**[6a]**$^+$
+ESI-MS (*m*/*z*)	1009.1013	1065.1655	1063.1493	1085.1317	1075.1478
^{31}P NMR					
δ_1	61.0	59.0	56.2	56.3 61.0	57.3
δ_2	40.3	40.0	41.1	45.9 40.7	40.0
δ_3	37.5	38.8	38.1	37.5 36.6	37.0
J_{12}, J_{13}, J_{23} (Hz)	30, 30, 304	30, 30, 318	30, 30, 313	30, 30, 300 30, 30, 311	30, 30, 315
Voltammetry					
$E_{1/2}$ (Ru^{III}/Ru^{II}) (mV)	+804	+792	+790	+788	+824

Table 3. Properties of Ru(III)−Dithioether Complexes **[2b]**$^{2+}$−**[6b]**$^{2+}$

	[2b]$^{2+}$	**[3b]**$^{2+}$	**[4b]**$^{2+}$	**[5b]**$^{2+}$	**[6b]**$^{2+}$
UV−Vis					
λ_{max} (nm)	690	682	697	692	n/d[a]
ϵ (M^{-1} cm^{-1})	3800	2700	2500	2200	
EPR					
g_1	2.09	2.08	2.09	2.09	2.09
g_2	2.04	2.03	2.05	2.05	2.05
g_3	2.03	2.02	2.02	2.03	2.03

[a] n/d = not determined due to solubility limitations.

1,2-dibromoethane. In this reaction, the ruthenium-containing complex, **[1a]**$^-$, is two electrons more reduced than in the electrochemical synthesis. Likewise, the 1,2-dibromoethane is two electrons more oxidized than ethylene. From the chemical synthesis, single crystals of **[2a]**$^+$ as the bromide salt were obtained for X-ray analysis.

Characterization. The spectroscopic properties of **[2a]**$^+$−**[6a]**$^+$ and **[2b]**$^{2+}$−**[6b]**$^{2+}$ are summarized in Tables 2 and 3, respectively. The +ESI-MS of **[2a]**$^+$ displays a parent ion peak at $m/z = 1009.1013$, which is within experimental error of the theoretical value of 1009.1018. The observed isotopic envelope well reproduces the theoretical envelope, which is characteristic of ruthenium, Figure 4. As shown in Table 2 and Figures S1−S4, the +ESI-MS spectra of **[3a]**$^+$−**[6a]**$^+$ also show the expected parent ion peaks within 1 ppm.

The ^{31}P NMR spectrum of **[2a]**$^+$ shows chemical shift values of $\delta_1 = 61.0$, $\delta_2 = 40.3$, and $\delta_3 = 37.5$ with coupling constants of $J_{12} \approx J_{13} \approx 30$ Hz and $J_{23} = 304$ Hz. This is consistent with three phosphorus donors arranged in a meridional fashion about an octahedral Ru(II) ion.[18,26,27] The ^{31}P NMR spectra of **[3a]**$^+$−**[6a]**$^+$ show coupling constants and isomeric shift values that are very close to those of **[2a]**$^+$. The ^{31}P NMR spectrum of **[5a]**$^+$ is unique, as it shows two sets of resonances with nearly equal intensities. This is attributed to the presence two diastereomers from the nonselective addition of unsymmetrical styrene to **[1c]**$^+$. Notably, only one set of peaks is observed for **[3a]**$^+$ indicating that either 1-hexene adds selectively or that the diastereormers cannot be resolved due to the similarities of their magnetic environments.

The oxidized complex, **[2b]**$^{2+}$, owes its green color to a charge-transfer band at 690 nm. A similar band is observed in the other oxidized complexes, **[3b]**$^{2+}$−**[5b]**$^{2+}$, which each display a single absorbance band in the visible region in the range of 682−697 nm. On the basis of their energies and molar absorptivities, these bands are assigned as thiolate-to-metal charge-transfer bands. Since **[6b]**$^{2+}$ precipitated from solution, no absorbance maximum was measured.

The EPR spectrum of a frozen acetonitrile solution of **[2b]**$^{2+}$ was recorded at 77 K in an EPR Suprasil quartz dewar, Figure 5. The spectrum of **[2b]**$^{2+}$ reveals a rhombic signal with $g_1 = 2.09$, $g_2 = 2.04$, and $g_3 = 2.03$, consistent with an $S = 1/2$ spin system. However, the g values cannot be attributed to Ru(III) by simple rotational relationships and spin−orbit coupling.[28] Additionally, attempts to model the g values using the approach of Taylor developed for a d^5 low-spin heme iron does not yield physically reasonable results.[29] This complexity is attributed to the high covalency of the Ru−S bond which makes assignment of the oxidation state difficult. In fact, the observed g values are similar to those observed for metal-coordinated thiyl radicals.[5] The EPR spectra of **[3b]**$^{2+}$−**[6b]**$^{2+}$ are all rhombic with g values similar to those of **[2b]**$^{2+}$.

X-ray Crystallographic Analysis. The structure of **[2a]-Br** has been determined by single-crystal X-ray techniques. Details of the data collection and refinement are presented in Table 1. Complex **[2a]Br** crystallizes with a 3/4 occupancy chlorobenzene solvate in the asymmetric unit. An ORTEP[30] view of the cation is presented in Figure 6, with selected bond distances and angles listed in Table 4.

The ruthenium ion of **[2a]Br** sits in pseudo-octahedral P_3S_3 donor environment. The phosphorus and sulfur donors arrange in a meridional fashion, as seen in related complexes. The thioether sulfur donors S2 and S3 are bridged by the ethylene linker, while S1 is a thiolate donor. The Ru−S1 bond length is 2.3856(9) Å and is close to previously reported Ru−$S_{thiolate}$ bonds.[18,27,31] The Ru−S thioether bond lengths for Ru−S2 and Ru−S3 are 2.3749(9) and 2.3365(9) Å, respectively. These values are slightly shorter than the previously reported values of Ru−S2 and Ru−S3 of 2.406-(1) and 2.358(1) Å, respectively, in **[7a]Cl**.[18] This decrease in bond length can be attributed to release of geometrical constraint due to formation of a five-member ring as opposed

(26) Dilworth, J. R.; Zheng, Y. F.; Lu, S. F.; Wu, Q. J. *Transition Met. Chem.* **1992**, *17*, 364−368.
(27) Dilworth, J. R.; Lu, C. Z.; Miller, J. R.; Zheng, Y. F. *J. Chem. Soc. Dalton Trans.* **1995**, 1957−1964.
(28) Palmer, G. Electron Paramagnetic Resonance of Metalloproteins. In *Physical Methods in Bioinorganic Chemistry: Spectroscopy and Magnetism*; Que, L., Jr., Ed.; University Science Books: Sausalito, CA, 2000.
(29) Taylor, C. P. S. *Biochim. Biophys. Acta* **1977**, *491*, 137−149.
(30) Farrugia, L. J. *J. Appl. Crystallogr.* **1997**, *30*, 565.
(31) Sellmann, D.; Shaban, S. Y.; Heinemann, F. W. *Eur. J. Inorg. Chem.* **2004**, 4591−4601.

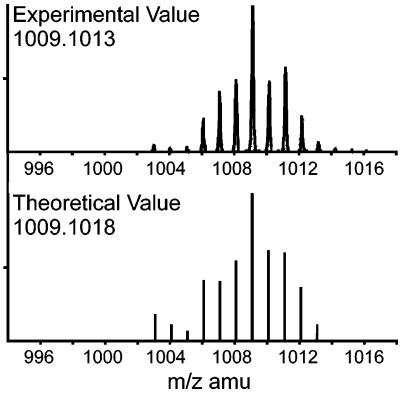

Figure 4. Experimental (top) and theoretical (bottom) isotopic distribution of parent ion peak in the +ESI-MS of **[2a]**$^+$ in acetonitrile.

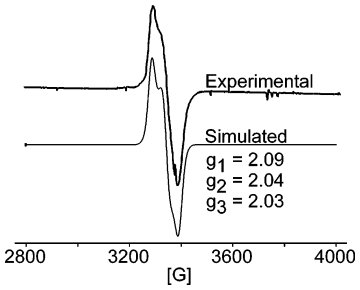

Figure 5. Experimental (top) and simulated (bottom) EPR spectrum of **[2b]**$^{2+}$ at 77 K. Experimental conditions: microwave frequency of 9.6011 GHz, microwave power of 1.978 mW, modulation frequency of 100 kHz, modulation amplitude of 10 G. Line widths for SIMPOW6 simulated spectrum : $W_x = 32$ G, $W_y = 39$ G, $W_z = 37$ G.

to a four-member ring in the methylene-bridged thioether. The carbon sulfur bond lengths for S(2)−C(55) and S(3)−C(56) are 1.836(4) and 1.843(4) Å, respectively. The Ru−P distances range from 2.3290(9) to 2.3965(10) Å and are comparable to previously reported Ru−P values in related systems.[18,27]

Discussion

Oxidation of the formally Ru(III)−trithiolate complex **1b** in the presence of alkenes has been shown to result in C−S bond formation and isolation of Ru(II)−dithioether products, **[2a]**$^+$−**[6a]**$^+$. On the basis of previous DFT investigations, the oxidized intermediate **[1c]**$^+$ is best described as having a singlet, diradical ground state with significant Ru(II)−dithiyl radical contributions.[16] Since the unpaired electrons of **[1c]**$^+$ are in nearly orthogonal orbitals, disulfide formation is slow. As such, **[1c]**$^+$ has a suitable lifetime to promote addition of unsaturated hydrocarbons across interligand cis-sulfur sites, Scheme 2. Addition of alkenes yields stable dithioether/thiolate Ru(II) complexes. These results provide definitive evidence for the addition of alkenes to a metal-coordinated thiyl radical. Interestingly, no evidence of H-atom abstraction has been observed, even when styrene was added to the reaction mixture. The addition of alkenes to **[1c]**$^+$ is consistent with the previously reported addition of methyl ketones.[17] Addition of the enol tautomer, Scheme 2, proceeds as an alkene addition. However, deprotonation, by adventious base or **1b**, results in cleavage of one of the C−S bonds to yield the observed monothioether products.

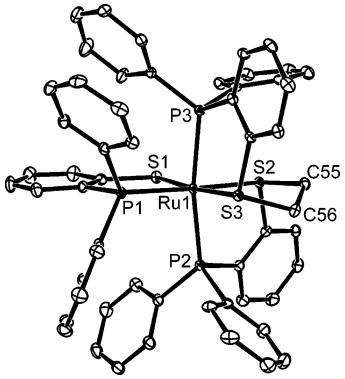

Figure 6. ORTEP representation of the cation of **[2a]Br** showing 30% probability displacement ellipsoids and partial atom-numbering scheme. H atoms and solvent molecule are omitted.

Table 4. Selected Bond Distances (Å) and Bond Angles (deg) of **[2a]Br**

Ru1−S1	2.3856(9)	S1−Ru1−P1	85.88(3)
Ru1−S2	2.3749(9)	S2−Ru1−P2	83.36(3)
Ru1−S3	2.3365(9)	S3−Ru1−P3	85.55(3)
Ru1−P1	2.3290(9)	P1−Ru1−S2	172.87(3)
Ru1−P2	2.3965(10)	S1−Ru1−S3	173.73(3)
Ru1−P3	2.3648(9)	P2−Ru1−P3	168.81(3)
S2−C55	1.836(4)	S2−Ru1−S3	87.71(3)
S3−C56	1.843(4)	C55−S2−Ru1	104.52(12)
C55−C56	1.510(5)	C56−S3−Ru1	103.59(12)

Scheme 2

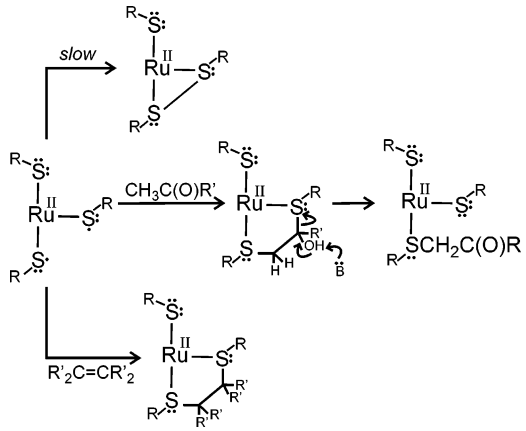

Previously, Stiefel and co-workers reported the interligand alkene addition across cis-sulfur sites upon oxidation of nickel dithiolenes with subsequent alkene dissociation upon reduction.[11] This intriguing result offered promise for the use of nickel dithiolenes for redox controlled reversible olefin binding as a means for olefin purification. However, subsequent studies by Geiger revealed the reaction was more complex.[12] Very recent studies by Fekl and co-workers indicate that the favored addition of alkenes to nickel dithiolenes is intraligand, leading to decomposition to dihydrodithiin and metal decomposition products.[13] Our family of complexes **[2a]**$^+$−**[6a]**$^+$ show the desired interligand addition sought in the earlier studies. However, as noted by Rothlisherger, Ru(II) dithioethers are not favorably reduced and therefore do not facilitate C−S bond cleavage.[32] In fact, complexes **[2a]**$^+$−**[6a]**$^+$ do not show any reduction

(32) Magistrato, A.; Maurer, P.; Fassler, T.; Rothlisherger, U. *J. Phys. Chem. A* **2004**, *108*, 2008−2013.

event within the solvent window. Further efforts are underway to develop a reversible system.

Acknowledgment. This research was supported in part by the National Science Foundation (CHE-0238137). Acknowledgment is made to the Donors of the American Chemical Society Petroleum Research Fund (43917-AC3) for partial support of this work. We thank the Kentucky Research Challenge Trust Fund for the purchase of CCD X-ray equipment and upgrade of our X-ray facility.

Supporting Information Available: +ESI-MS of **[3a]**$^{+}$−**[6a]**$^{+}$ in pdf format and crystallographic data for **[2a]Br** in CIF format (CCDC 649178). This material is available free of charge via the Internet at http://pubs.acs.org.

IC701078E